Chemistry Europe

AWARD

Nominate a Worthy Chemist Chemistry Europe Award

Subject:
chemistry for sustainability, energy, materials, environment

Consists of:
prize money amounting to EUR 10,000, certificate

Deadline:
November 1, 2022

Click here for more info & nomination

Energy Technology & Environmental Science

Synthesis and Performance Evaluation of $Na_{(2-x)}Li_xFeP_2O_7$ (x = 0, 0.6) Hybrid Cathodes

Jeffin James Abraham,[a] Hanan Tariq,[a] Rana Abdul Shakoor,*[a] Ramazan Kahraman,[b] and Siham Al-Qaradawi[c]

This study reports hybrid cathodes formation by cation substitution in which Li^+ substitution has been considered for Na^+ in the structure of $Na_{(2-x)}Li_xFeP_2O_7$ (x = 0, 0.6) to form $Na_{1.4}Li_{0.6}FeP_2O_7$ cathodes. $Na_{(2-x)}Li_xFeP_2O_7$ (x = 0, 0.6) cathodes were synthesized using the solid-state synthesis technique and characterized by various methods. The structural analysis (XRD, FE-SEM) indicates that the submicron-sized, phase pure, and crystalline materials having irregular morphology have been developed. Moreover, Li^+ substitution does not alter the triclinic parent structure of $Na_2FeP_2O_7$. Thermogravimetric analysis (TGA) shows that Li^+ substitution into $Na_2FeP_2O_7$ improves its thermal stability up to 550 °C with only ~5% weight loss. The electrochemical performance of $Na_2FeP_2O_7$ and $Na_{1.4}Li_{0.6}FeP_2O_7$ in both lithium (Li) and sodium (Na) half-cells is investigated using different electrochemical techniques. It is noticed that $Na_{1.4}Li_{0.6}FeP_2O_7$ is electrochemically active both in lithium (Li) and sodium (Na) cells with promising cyclability. However, compared with $Na_2FeP_2O_7$, $Na_{1.4}Li_{0.6}FeP_2O_7$ suffers from inferior electrochemical performance, which might be associated with the lattice distortion of $Na_2FeP_2O_7$ due to Li^+ substitution having a lower ionic radius than the Na^+. Considering $Na_2FeP_2O_7$ as a baseline material, a new hybrid $Na_{1.4}Li_{0.6}FeP_2O_7$ cathode has been developed, which can be used to synthesize other new cathode materials with improved performance.

1. Introduction

With effectively declining and polluting fossil fuel reserves, clean energy sources have been considered as a decent solution. Towards this direction, battery technology is an essential and promising clean energy source that contributes significantly to reduce environmental pollution. For the past few years, lithium-ion batteries (LIBs) have become one of the most essential and integral parts of our daily life. However, with the increasing trend of utilization of electronic devices such as hybrid electric vehicles (HEVs) and electric vehicles (EVs) using LIBs, there may be a rapid depletion in lithium reserves across the world, which can increase the production cost of lithium metal considerably.[1–3] Sodium-ion batteries (SIBs) have emerged as a valuable replacement for the energy storage market with its low price and large-scale availability.[4–6] Other than its abundant nature, sodium displays similar electrochemical properties with its lithium counterpart, making it an excellent substitute for lithium counterpart.[6–9] SIBs had their beginnings in high-temperature cells like $Na/NiCl_2$ and Na–S, which were commercialized into grid-scale energy storage systems (ESS) and some other applications.[10–14] Although SIBs bring in an adequate cost-efficient replacement to its lithium counterpart, these carry some visible drawbacks leading to overshadow their good advantages. The sodium ions (Na^+) has a larger ionic radius (1.02 Å) when compared to lithium ions (Li^+) (0.76 Å), leading to inadequate performance. The performance of SIBs is also suffering from sluggish ionic transportation, the formation of undesired phases, and lack of phase stability.[7,8,15,16] Moreover, sodium has a higher standard potential than lithium and is also significantly more massive than lithium leading to lower energy densities, contributing to plague SIBs.[8]

Since the discovery of SIBs, various cathode materials have been developed and thoroughly investigated. Among those phosphates, pyrophosphate and fluorophosphate cathode materials display appealing characteristics. These families mainly include $NaFePO_4$,[17] $Na_2FeP_2O_7$,[18] $Na_2VP_2O_7$,[19] $Na_2Fe_{0.5}Mn_{0.5}P_2O_7$,[20] $Na_4MnV(PO_4)_3$,[7] $Na_4Fe_3(PO_4)_2(P_2O_7)$[21] and $Na_3V_2(PO_4)_2F_3$.[22] These cathode materials have been comprehensively studied throughout the years and are recommended for energy storage applications because of low synthesizing cost, the formation of stable crystal structure, enhanced thermal stability, comparatively better energy density, and improved safety.[1,7,18,20,22–27] Among the family of pyrophosphate, the $Na_2FeP_2O_7$ is a promising cathode material demon-

[a] J. J. Abraham, H. Tariq, Dr. R. A. Shakoor
Center for Advanced Materials (CAM), Qatar University, P. O. Box 2713, Doha, Qatar
Tel: + 974-4403-6867
E-mail: shakoor@qu.edu.qa
[b] Prof. R. Kahraman
Department of Chemical Engineering, College of Engineering, Qatar University, P. O. Box 2713, Doha, Qatar
[c] Prof. S. Al-Qaradawi
Department of Chemistry & Earth Sciences, College of Arts and Science (CAS), Qatar University, P. O. Box 2713, Doha, Qatar

Supporting information for this article is available on the WWW under https://doi.org/10.1002/slct.202003658

strating a decent reversible capacity ~90mAhg^{-1}, an excellent rate capability, and decent thermal stability.[18] Like other SIBs, $Na_2FeP_2O_7$ also displays sparse energy density, and lithium substitution in this pyrophosphate structure may be a possible way to overcome the drawbacks of $Na_2FeP_2O_7$ cathode material.

Numerous techniques, such as doping,[28] surface coatings,[29] transition metal substitution,[30,31] composite structure formation,[32], and particle size reduction,[33], etc. have been suggested to modify the properties of the various cathode materials. Kim et al.[4] studied the effect of lithium substitution in the $Na_{1.0}Li_{0.2}Ni_{0.25}Mn_{0.75}O_2$ cathode material, which displayed a specific capacity of ~95mAhg^{-1}, good cyclic performance, and an excellent rate capability. The improved electrochemical performance was attributed to the presence of lithium in the crystal structure. Similarly, many other groups have also reported the enhanced electrochemical performance of various families of cathode materials due to lithium substitution.[34–36]

In the present research work, we propose the partial substitution of sodium with lithium in the crystal structure of $Na_{2-x}Li_xFeP_2O_7$ (where x = 0, 0.6). The partial substitution of lithium was undertaken by employing a conventional solid-state synthesis process reported by Kim et al..[18] The effect of Li^+ substitution on the structural, thermal, and electrochemical performance of $Na_{2-x}Li_xFeP_2O_7$ (where x = 0, 0.6) was conducted employing various techniques. The electrochemical performance and intercalation/deintercalation of Li^+/Na^+ into/from the $Na_{2-x}Li_xFeP_2O_7$ (where x = 0, 0.6) was conducted in both lithium and sodium half-cells. A comparative analysis of $Na_2FeP_2O_7$ and $Na_{1.4}Li_{0.6}FeP_2O_7$ indicates that $Na_{1.4}Li_{0.6}FeP_2O_7$ demonstrates improved thermal stability; however, its electrochemical performance is not enhanced as compared to the $Na_2FeP_2O_7$ as aimed. However, more investigations can be undertaken to figure out the origin of this drop in the electrochemical performance by lithium substitution in the pyrophosphate structure.

2. Results and discussion

Figure 1 (a) shows the XRD patterns of $Na_{2-x}Li_xFeP_2O_7$ (where x = 0, 0.6). The XRD patterns reveal that the synthesized samples have high crystallinity without any impurities suggesting the formation of pure phase materials. This is in line with the previous study, as reported by Kim et al..[18] In $Na_{1.4}Li_{0.6}FeP_2O_7$, two more peaks are observed in the 2Θ range of 25–40° range due to the presence of lithium into the structure of $Na_2FeP_2O_7$ without altering the parent crystal structure of $Na_2FeP_2O_7$. The $Na_{1.4}Li_{0.6}FeP_2O_7$ is identified as phase pure as the additionally observed peaks in $Na_{1.4}Li_{0.6}FeP_2O_7$, from the range 25–40°, are also identified in the XRD spectra of $Li_2FeP_2O_7$, as reported in previous studies.[37–39] Since the synthesis procedure is consistent with that of Kim et al., the synthesized $Na_2FeP_2O_7$ is in line with the triclinic structure and can be attributed to the *P1* group.[18] $Li_2FeP_2O_7$ displays a monoclinic structure, as reported in the previous studies.[37,38,40] The crystal structure of the synthesized pure $Na_2FeP_2O_7$ material constructed using Vesta software is shown in Figure 1 (b). As mentioned in the previous reports,[18] there are eight Na sites in the unit cell. Na ion migration occurs due to channels created by the metal and pyrophosphate polyhedra connecting with each other and corner-sharing. Likewise, the newly synthesized $Na_{1.4}Li_{0.6}FeP_2O_7$ shares a similar crystal structure (Figure 1 (c)). However, instead of having 8 Na sites, the Li substituted sample has a mixture of Na and Li in its unit cell. It shares similar positioning of metal and pyrophosphate polyhedra, as in the case of $Na_2FeP_2O_7$.

Figure 2 shows the FE-SEM images for $Na_{2-x}Li_xFeP_2O_7$ (where x = 0, 0.6) cathodes. The developed materials show a well-defined structure and have irregular particle morphology (Figure 2 (a, b)). Some accumulation of particles can also be seen, which can be ascribed to the ball milling effect. The $Na_2FeP_2O_7$ has a particle size ranging ~100 nm–300 nm and the $Na_{1.4}Li_{0.6}FeP_2O_7$ particle size ranges from ~80 nm to 200 nm as calculated by the Image J software.[18,41] The reduction in

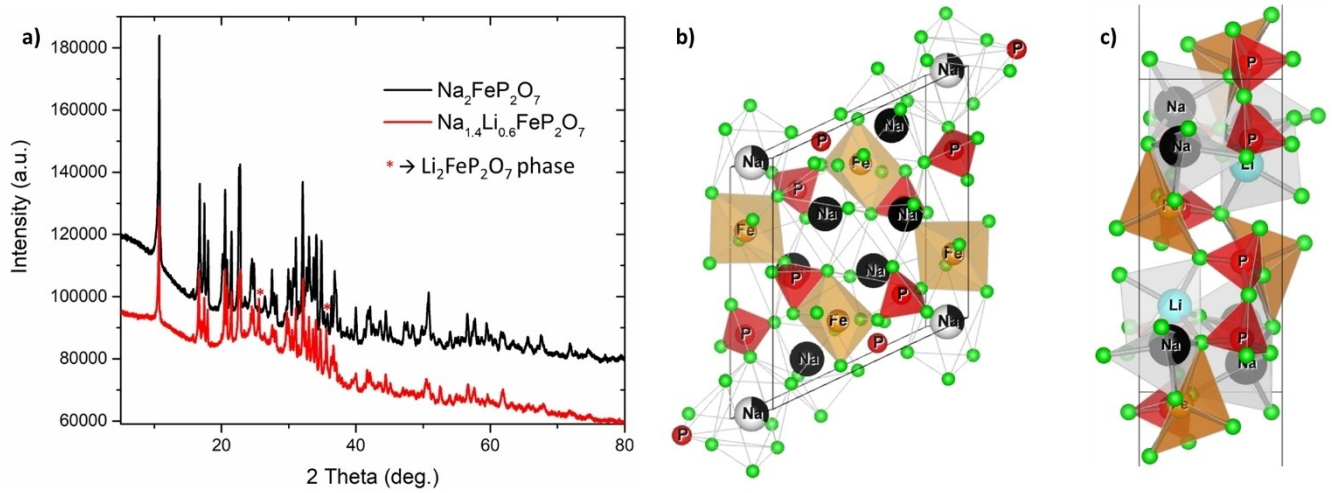

Figure 1. (a) XRD spectra of $Na_2FeP_2O_7$ and $Na_{1.4}Li_{0.6}FeP_2O_7$, (b) crystal structure of $Na_2FeP_2O_7$ and (c) proposed crystal structure of $Na_{1.4}Li_{0.6}FeP_2O_7$.

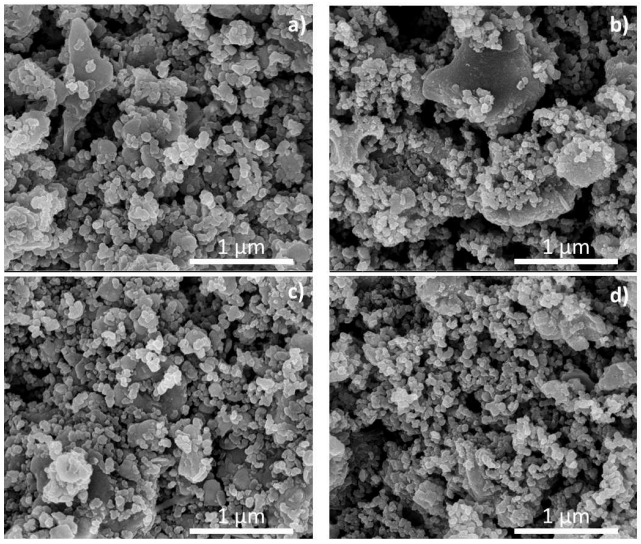

Figure 2. FE-SEM images of the synthesized $Na_{2-x}Li_xFeP_2O_7$ (where x = 0, 0.6) cathodes, (a) pristine $Na_2FeP_2O_7$, (b) pristine $Na_{1.4}Li_{0.6}FeP_2O_7$ and (c) carbon coated $Na_2FeP_2O_7$, (d) carbon coated $Na_{1.4}Li_{0.6}FeP_2O_7$.

particle size of $Na_{1.4}Li_{0.6}FeP_2O_7$ can be attributed to the metal substitution or dopping effect.[18,20] The larger particle size of $Na_{2-x}Li_xFeP_2O_7$ (where x = 0, 0.6) can be attributed to the inherent characteristics of the solid-state synthesis process. Furthermore, the carbon coating of the $Na_{2-x}Li_xFeP_2O_7$ (where x = 0, 0.6) has resulted in a reduction in the particle size (Figure. 2 (c, d), which can be ascribed to the ball milling effect.[38,42,43]

Figure 3 shows the TGA curves of the carbon-coated $Na_{2-x}Li_xFeP_2O_7$ (where x = 0, 0.6) cathodes performed under N_2 atmosphere. Both samples display excellent thermal stability when heated to 550 °C. As a comparison, $Na_{1.4}Li_{0.6}FeP_2O_7$ shows slightly better weight retention as compared to $Na_2FeP_2O_7$. There is a weight loss of around ~7% for the $Na_2FeP_2O_7$ sample

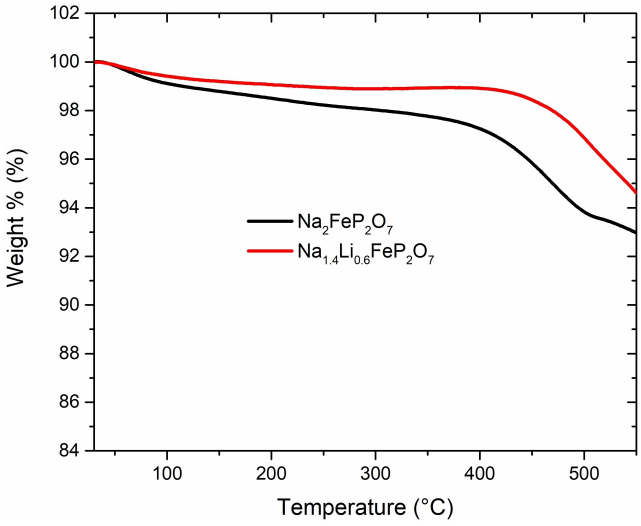

Figure 3. TGA analysis of carbon coated $Na_{2-x}Li_xFeP_2O_7$ (where x = 0, 0.6) cathodes under N_2 atmosphere.

when heated to 550 °C, whereas the $Na_{1.4}Li_{0.6}FeP_2O_7$ sample shows a weight loss of ~5% till 550 °C. The $Na_2FeP_2O_7$ demonstrates a gradual reduction in weight loss with increasing temperature, whereas the $Na_{1.4}Li_{0.6}FeP_2O_7$ sample shows better thermal stability until ~400 °C without significant weight loss. This shows that the substitution of sodium with lithium in the $Na_{2-x}Li_xFeP_2O_7$ (where x = 0, 0.6) cathodes has resulted in a slight improvement in the thermal stability. The thermal stability observed in $Na_{1.4}Li_{0.6}FeP_2O_7$ is consistent with the previous reports for $Na_2FeP_2O_7$ and $Li_2FeP_2O_7$.[18,44]

The galvanostatic charge/discharge curves of $Na_{2-x}Li_xFeP_2O_7$ (where x = 0, 0.6) in Na and Li cells at different C rates are shown in Figure 4. The $Na_2FeP_2O_7$ demonstrates a similar charge/discharge capacity, as reported previously in the sodium cell.[18] A discharge capacity of 90mAh/g is achieved at 0.05 C rate, which decreases with increasing C rate (Figure 4 (a)) and reaches ~79mAh/g at 4 C, showing good rate performance. However, in comparison, $Na_2FeP_2O_7$ demonstrates an insufficient discharge capacity in Li cell (Figure 4 (b)), which can be ascribed to the formation of an unstable solid-electrolyte interface layer (SEI) on the cathode.[2,45] The first main observation in the Li cell is the lack of/smaller multi plateau Charge/discharge process, as observed in the Na cell. This can be identified as the insertion of Na^+ ions and Li^+ ions.[46] The second observation noticed is the discrepancy of capacities between Na cell and Li cell at different C rates. The capacities at C rates higher than C/10 are much lower and distinct in the Li cell as compared to that of the Na cell. This can be explained as a result of incomplete Na ion substitution for Li-ions, which in turn results in obstruction of Li-ions during the intercalation process, as demonstrated by Kosova et al..[46] Herein, at higher C rates, the Li intercalation/deintercalation process is impeded by incomplete Na ion substitutions. The Li-cell of the $Na_2FeP_2O_7$ shows the capacity of ~94mAh/g at 0.05 C and ~28mAh/g at 4 C.

The charge/discharge capacity of $Na_{1.4}Li_{0.6}FeP_2O_7$ at different C-rates in Na cells is shown in Figure 4 (c). In the case of the Na cell, it shows a similar multistep plateau-like its $Na_2FeP_2O_7$ counterpart. Since the Na ion is the predominant ion in this material, it displays similar properties to that of $Na_2FeP_2O_7$. However, comparing the discharge capacities, $Na_{1.4}Li_{0.6}FeP_2O_7$ shows much lower capacities at different C-rates. It offers a capacity of ~60mAh/g at 0.05 C and a capacity of ~13mAh/g at 4 C. The poor rate performance might be due to the interrupted movement of Li^+ due to lattice distortion and instability in the crystal structure due to the substitution of Li into the structure.[4,34,47] A stable structure is a requirement for good electrochemical performance. The inferior capacity of $Na_{1.4}Li_{0.6}FeP_2O_7$ in Na cell can be explained as a result of many different factors such as; (i) unstable structure during the intercalation/deintercalation, (ii) incomplete substitution of Li^+ resulting in lack of Na ion mobility during intercalation/deintercalation process and (iii) a decrease in the amount of active Na^+ which were replaced by Li^+ in the structure. Furthermore, the loss of irreversible capacity in the first cycle can be explained due to a combination of reasons like the occurrence of unwanted reactions because of electrolyte and

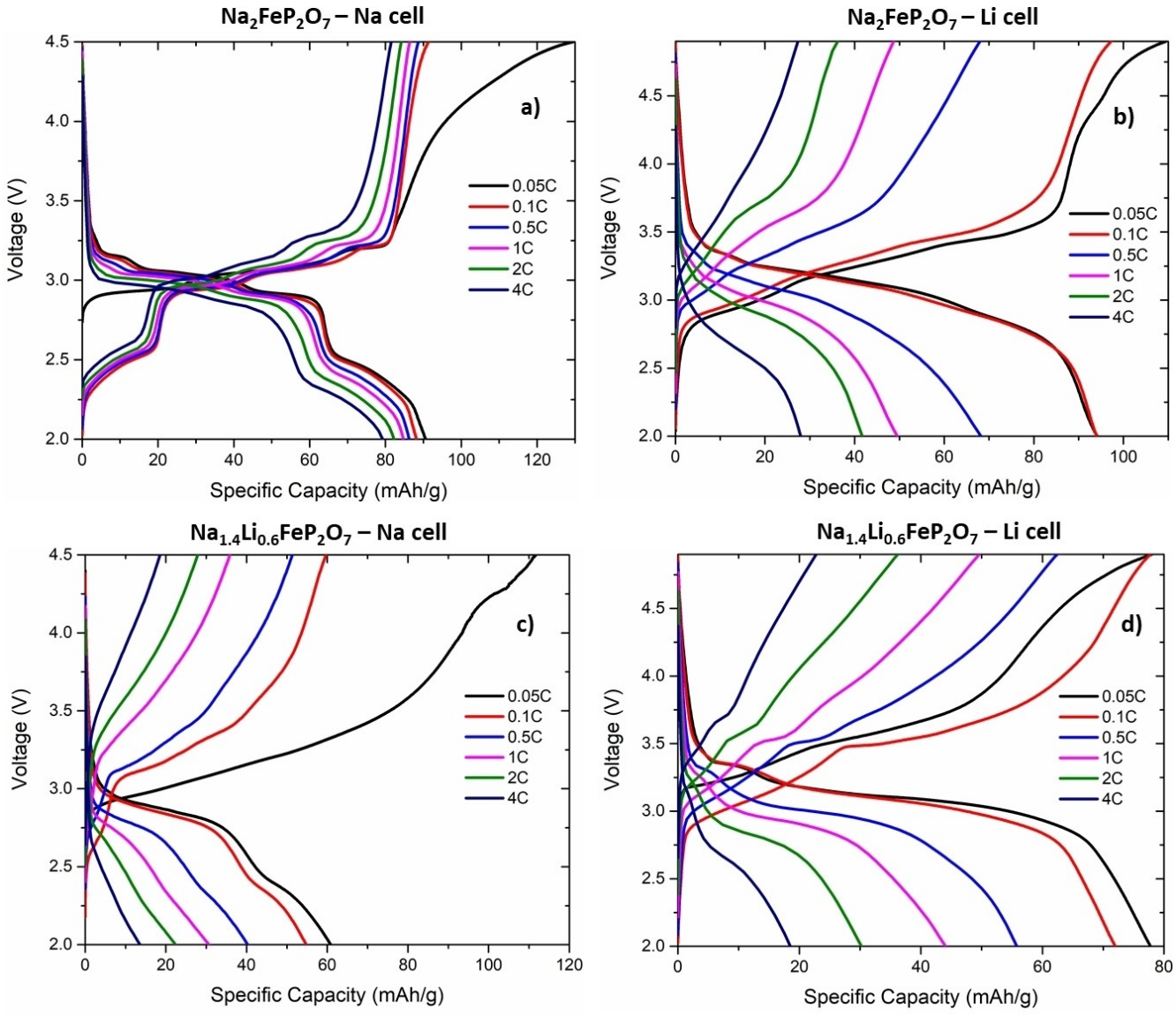

Figure 4. Galvanostatic charge/discharge; (a) $Na_2FeP_2O_7$ in Na cell, (b) $Na_2FeP_2O_7$ in Li cell, (c) $Na_{1.4}Li_{0.6}FeP_2O_7$ in Na cell and (d) $Na_{1.4}Li_{0.6}FeP_2O_7$ Li cell.

Na metal interaction and Na plating during the charging process.[4,48] The lack of broader charge/discharge plateaus further confirms the poor electrochemical performance of the $Na_{1.4}Li_{0.6}FeP_2O_7$ in Na cell.

On the other hand, $Na_{1.4}Li_{0.6}FeP_2O_7$ in the Li-cell shows at 0.05 C, a capacity of ~78mAh/g, and at 4 C offers a capacity of ~18mAh/g (Figure 4 (d)). The results observed in this case are similar to that of $Na_2FeP_2O_7$ in Li cell. The Li cell shows better performance as compared to the Na cell. Broad plateaus are observed in the discharge cycles. However, $Na_{1.4}Li_{0.6}FeP_2O_7$ faces rapid capacity loss at high C rates. With closer observations of the charge/discharge curves, a multi plateau charge and discharge are observed. This suggests a multiple-stage insertion/extraction of the Li^+ ions during the charge/discharge process. The Na substitution also plays a role in this sample, at high C rates, as seen from the curves lacking multi plateaus. To conclude, we can say that Li cell shows a lower capacity at all C rates when compared to $Na_2FeP_2O_7$ in sodium cell, which can be attributed to lattice distortion and unstable structure during intercalation/deintercalation. For more clarity, discharge capacities of $Na_2FeP_2O_7$ and $Na_{1.4}Li_{0.6}FeP_2O_7$ at the different C rates in Na Cell and Li cells are tabulated in Table 1. On comparing, it can be seen that $Na_{1.4}Li_{0.6}FeP_2O_7$ shows a rapid loss in capacity at high C rates, whereas the stable structure of the $Na_2FeP_2O_7$ samples leads to increased capacity and more stability at high C rates.

The rate capability of $Na_2FeP_2O_7$ and $Na_{1.4}Li_{0.6}FeP_2O_7$ are shown in Figure 5. $Na_2FeP_2O_7$ is a stable material in the Na cell as proven by previous studies and offers promising rate capability at different C-rates. The $Na_2FeP_2O_7$ material shows a capacity of ~90mAh/g at C/20 rate and shows excellent rate capability. In the case of the Li cell, $Na_2FeP_2O_7$ shows very high

Table 1. Comparison of discharge capacities of $Na_2FeP_2O_7$ and $Na_{1.4}Li_{0.6}FeP_2O_7$ and lithium and sodium cells.

Materials/C-rate	0.05 C (mAh g^{-1})	0.1 C (mAh g^{-1})	0.5 C (mAh g^{-1})	1 C (mAh g^{-1})	2 C (mAh g^{-1})	4 C (mAh g^{-1})
$Na_2FeP_2O_7$ Na-cell	90	88	86	85	82	79
$Na_2FeP_2O_7$ Li-cell	94	94	68	50	41	28
$Na_{1.4}Li_{0.6}FeP_2O_7$ Na-cell	60	54	40	30	22	13
$Na_{1.4}Li_{0.6}FeP_2O_7$ Li-cell	78	72	56	44	30	18

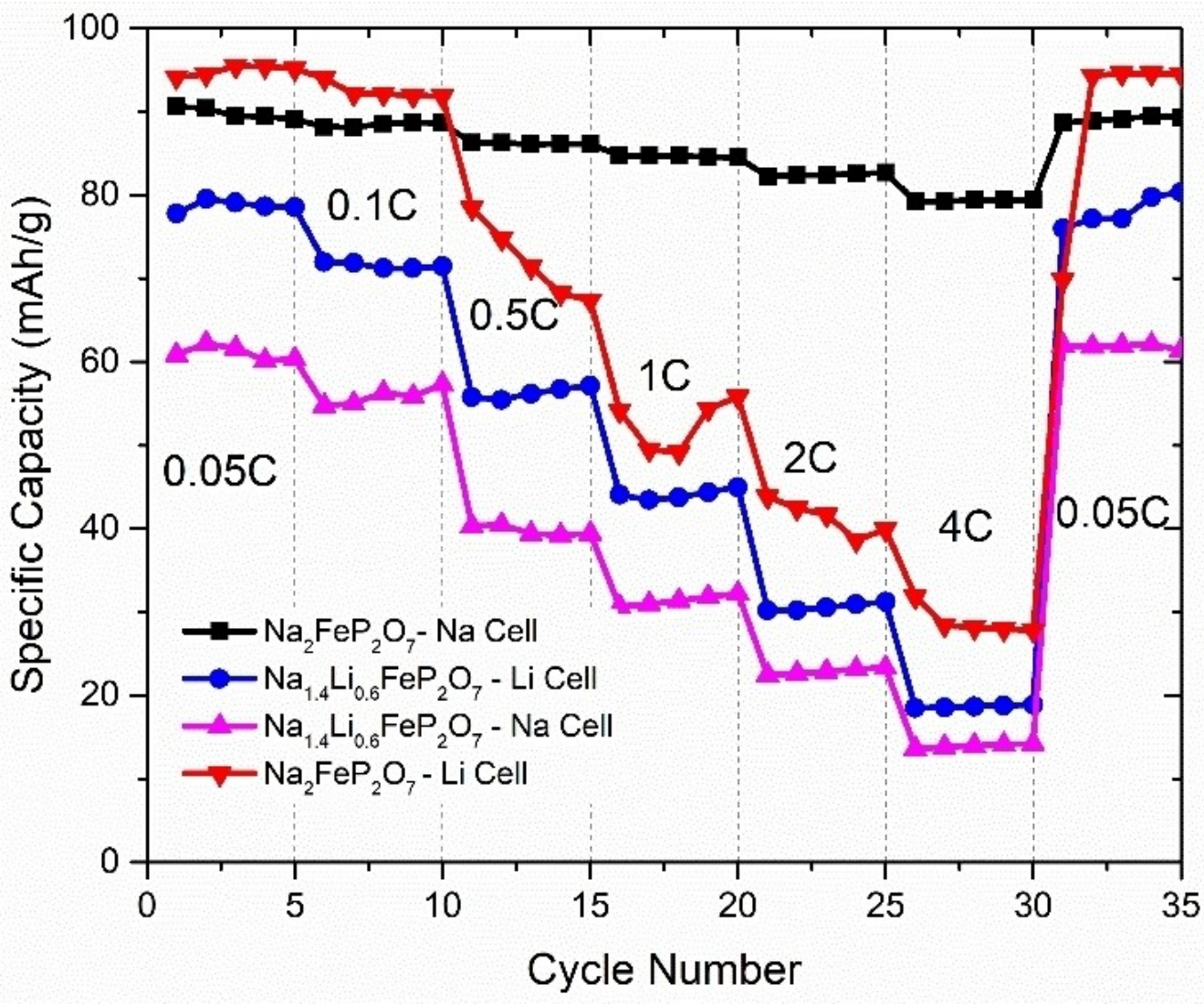

Figure 5. Rate capability comparison of $Na_2FeP_2O_7$ and $Na_{1.4}Li_{0.6}FeP_2O_7$ in Li and Na cells.

capacities at 0.05 C and 0.1 C. However, there is a rapid decrease in capacities at higher C rates. As stated earlier in the galvanostatic charge/discharge section, a lower amount of Li^+ ion insertion is one of the significant factors for the lower performance of $Na_2FeP_2O_7$ at higher C rates. However, the Li cell shows very good recoverability when re-cycled at C/20 rate. It offers a capacity of ~94mAh/g at C/20 rate and consistent recoverability.

Compared to the $Na_2FeP_2O_7$, the $Na_{1.4}Li_{0.6}FeP_2O_7$ shows an overall lower capacity at all C-rates both in the Na cell and Li cells. In Li cell, at C/20 rate, $Na_{1.4}Li_{0.6}FeP_2O_7$ shows a capacity of ~80mAh/g and shows a rapid capacity fading with increasing C rates, which is inferior to $Na_2FeP_2O_7$. The presence of lattice distortion due to the substitution of Li into the structure may be the reason for its inferior electrochemical performance. The Na cell for $Na_{1.4}Li_{0.6}FeP_2O_7$ sample shows a capacity of ~60mAh/g at C/20 rate, which is even inferior to the Li cell.

The presence of Li in a substituted sample is a deterrent at high C rates. Finally, after completing 30 cycles, the $Na_{(2-x)}Li_xFeP_2O_7$ (x = 0, 0.6) shows good recoverability both in Li and Na cells at C/20 rate. Overall, the best performance is observed in the Na cell for $Na_2FeP_2O_7$, which displays high capacity at all the C rates tested.

Figure 6 compares the cycling performance of $Na_2FeP_2O_7$ and $Na_{1.4}Li_{0.6}FeP_2O_7$ at C/20 rate for 50 cycles in the Na cell and Li cell and its coulombic efficiencies. $Na_2FeP_2O_7$ shows a decent initial discharge capacity of ~90mAh/g. A slow capacity fade can be seen throughout 50 cycles, as reported previously.[18] For an exact comparison, $Na_2FeP_2O_7$ in Li cell was also tested to better understand the effect of Li substitution in $Na_2FeP_2O_7$ cathode materials. The Li cell for $Na_2FeP_2O_7$ material shows an excellent capacity of ~92 mAh/g at C/20 rate. In comparison to $Na_2FeP_2O_7$ in sodium cell, it shows much better capacity retention with a capacity retention of up to 96%. In terms of cycling at C/20 rate, the Li cell for $Na_2FeP_2O_7$ displays better capacity and reversibility over 50 cycles. The coulombic efficiencies of the $Na_2FeP_2O_7$ Na cells show a fluctuation and can be attributed to the slow capacity fade observed throughout 50 cycles. It is, however, noted that the Li cell maintains stable efficiency values as compared to the Na cell.

In the $Na_{1.4}Li_{0.6}FeP_2O_7$ sample, both Li-cell and Na-cell show good cyclability but at a lower capacity as compared to $Na_2FeP_2O_7$. The Li-cell shows a capacity of ~85mAh/g, and the Na-cell shows a capacity of ~65mAh/g without any visible capacity fade with continuous cycling. However, $Na_{1.4}Li_{0.6}FeP_2O_7$ in Li cell shown some capacity fluctuations during cycling, but the overall average capacity remains almost constant through 50 cycles. To summarize, it can be commented that there is no significant loss of capacity for $Na_{1.4}Li_{0.6}FeP_2O_7$ both in Na cell and Li cells during 50 cycles suggesting good cyclability and reversibility of this material at C/20 rate. In the case of $Na_{1.4}Li_{0.6}FeP_2O_7$, both Na and Li cells show stability in their coulombic efficiencies throughout 50 cycles, further confirming their stable performance during cycling.

The GITT curves of $Na_2FeP_2O_7$ and $Na_{1.4}Li_{0.6}FeP_2O_7$ in Li and Na cells are shown in Figure 7. All GITT measurements were performed at C/20 rate between 2.0–4.5 V. GITT curve for $Na_2FeP_2O_7$ in the Na cell (Figure 7 (a)) indicates that during the initial stage of charging from 2.0 V to 3.25 V, the cell displays almost no polarization because of efficient and more comfort-

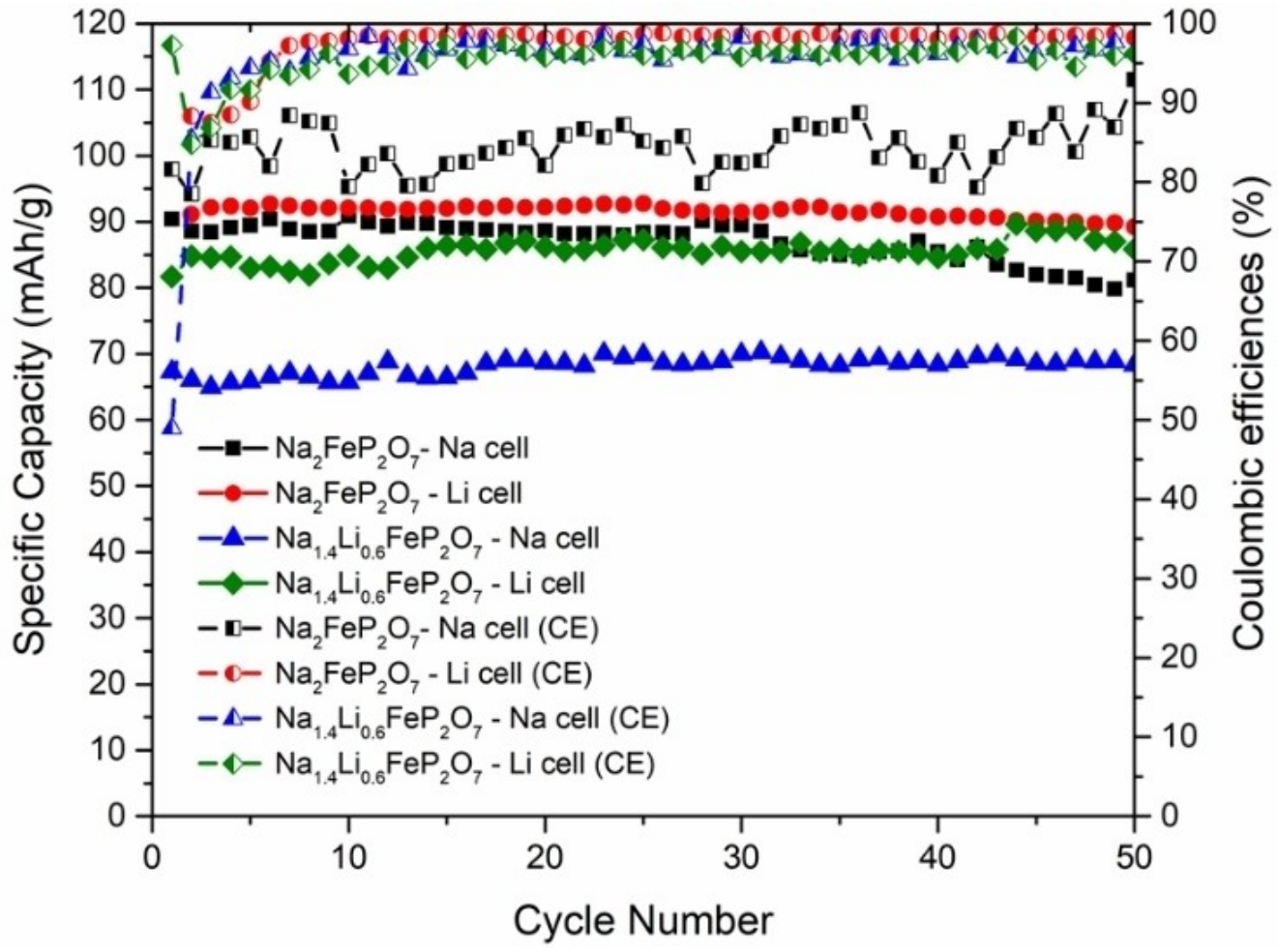

Figure 6. Cycling performance of $Na_2FeP_2O_7$ and $Na_{1.4}Li_{0.6}FeP_2O_7$ in Li and Na cells at 0.05 C rate and its coulombic efficiencies.

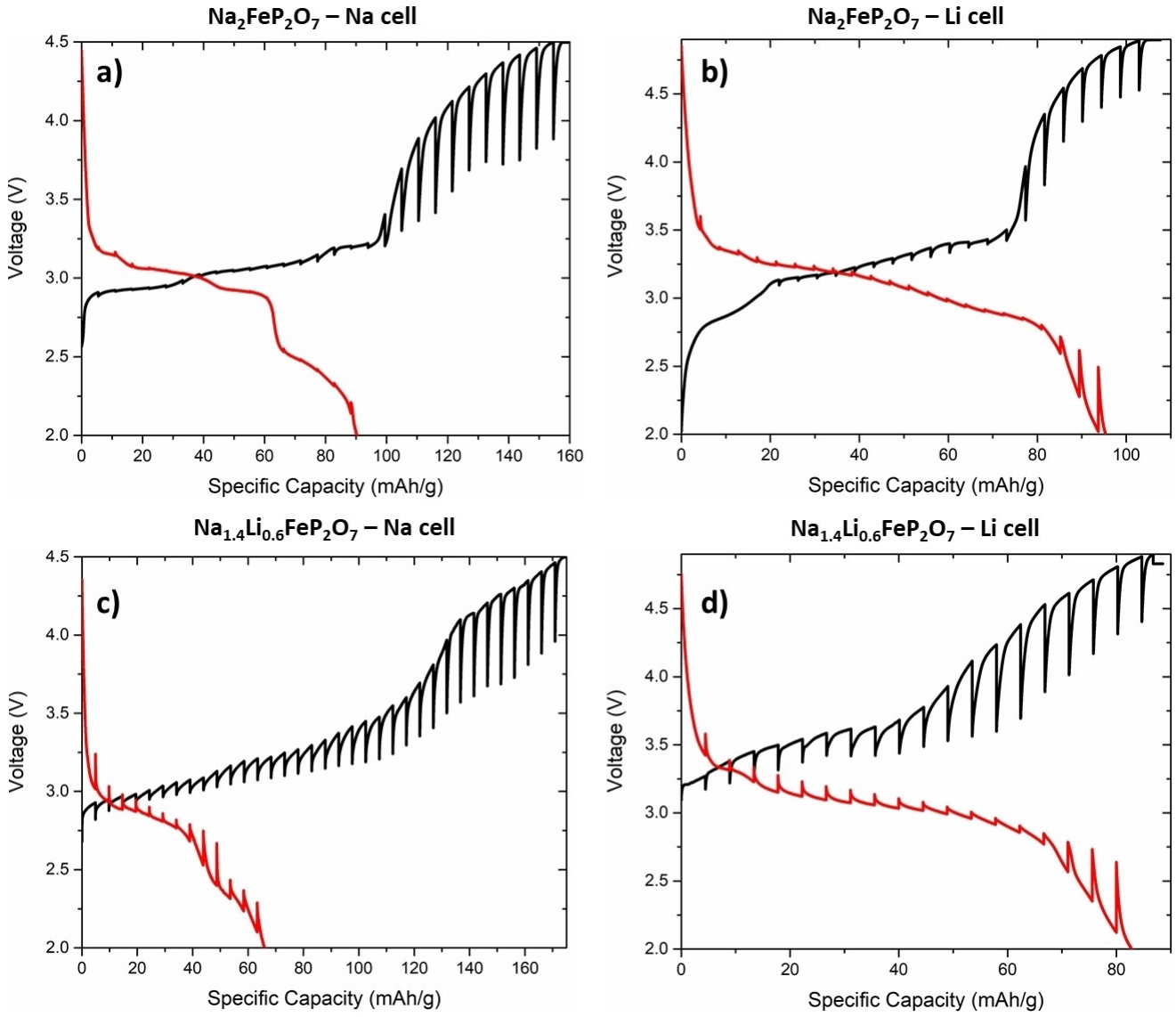

Figure 7. GITT curves at 0.05 C for a) $Na_2FeP_2O_7$ - Na cell, b) $Na_2FeP_2O_7$ - Li cell, c) $Na_{1.4}Li_{0.6}FeP_2O_7$ - Na cell and d) $Na_{1.4}Li_{0.6}FeP_2O_7$ - Li cell.

able Na^+ deintercalation from the host structure. However, during the later stage of charging from 3.25 V to 4.5 V, the material displays high polarization, which might be due to sluggish Na^+ deintercalation from the structure, also consistent with the previous studies.[18] As a result, the Na cell displays a charge capacity of ~160mAh/g. The origin of high charge capacity in the first cycle has been explained in the galvanostatic charge/discharge section. During discharging, the cell displays minimum polarization during the whole discharge range exhibiting a discharge capacity of ~90mAh/g, which shows the efficient intercalation of Na^+ into the host structure during the discharge process. The GITT behavior of $Na_2FeP_2O_7$ in Li cells is shown in Figure 7 (b). A similar trend is observed, as noticed in the Na cell. However, during discharging, there is a small polarization when compared to Na cell. Overall, the polarization trend during charging and discharging is very similar to the Na cell.

GITT curves of $Na_{1.4}Li_{0.6}FeP_2O_7$ in both Na cell and Li cells are presented in Figure 7 (c, d). When compared with $Na_2FeP_2O_7$ in Na and Li cells, large polarization is observed during charging and discharging, indicating sluggish kinetics for the migration of Li^+. It can be observed that initially, $Na_{1.4}Li_{0.6}FeP_2O_7$ shows low polarization both in the Na cell and Li cells, which increases when reaching higher voltage. This indicates that the migration of Na^+/Li^+ is initially easy to extract from the host structure, which becomes difficult with increasing voltage suggesting impeded ionic movement in the host structure. During the discharge, the material also displays high polarization in both the cells, unlike $Na_2FeP_2O_7$. The presence of lithium in the structure might have distorted the crystal structure and thus hindering the Na^+/Li^+ movement, which resulted in high polarization.

Figure 8 shows the cyclic voltammetry curves of $Na_2FeP_2O_7$ and $Na_{1.4}Li_{0.6}FeP_2O_7$ in Li and Na cells. Figure 8 (a) shows the CV

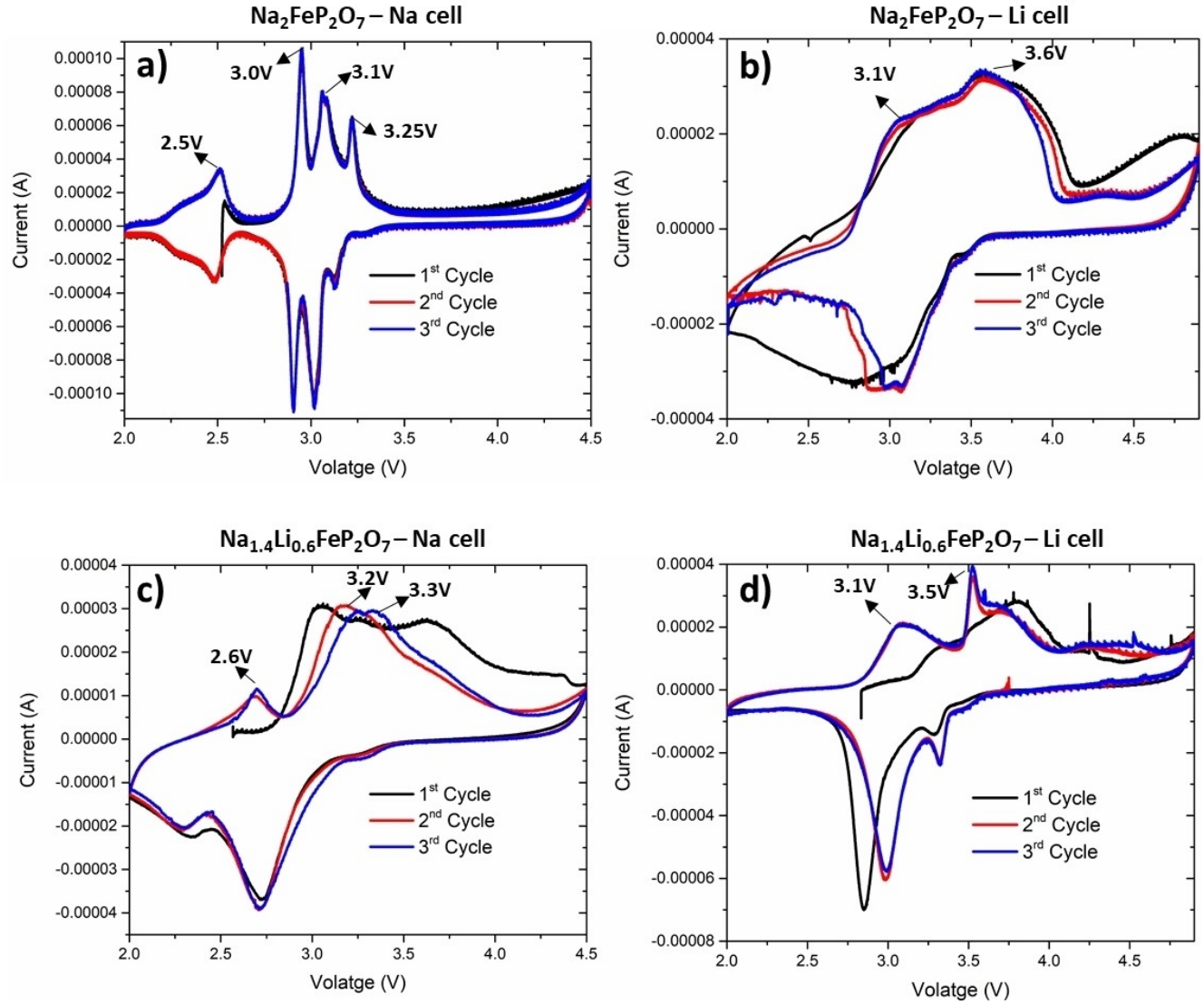

Figure 8. Cyclic Voltammetry curves measured at 0.05 mV/s for a) $Na_2FeP_2O_7$ - Na cell, b) $Na_2FeP_2O_7$ - Li cell, c) $Na_{1.4}Li_{0.6}FeP_2O_7$ - Na cell and d) $Na_{1.4}Li_{0.6}FeP_2O_7$ - Li cell.

for $Na_2FeP_2O_7$ in a Na cell. Four clear and distinct peaks are observed in the CV at around 2.5 V, 3.0 V, 3.1 V, and 3.25 V. These CV peaks can be related to the removal of Na^+ from different sodium sites available in the structure, which are operated at various activation energies and voltages. This can also be regarded as the effect of structural rearrangement or the Na^+ ordering.[18,49] This matches with the previously reported data for $Na_2FeP_2O_7$.[18,49] . As reported in previous studies, the peak at 2.5 V can be correlated with Na removed from pyrophosphate lattice due to its thermodynamic and kinetic accessibility, and all other peaks are related to the removal of Na at specific activation energies, with each one differing from other based on intercalation/deintercalation pathways.[18,50,51] The Li cell for $Na_2FeP_2O_7$ displays a very different CV pattern; during charging, two quite broad peaks are observed at 3.1 V and 3.6 V compared with the Na cell. The existence of these peaks can be regarded as the effect of the extraction of lithium from different sites at different voltages.

$Na_{1.4}Li_{0.6}FeP_2O_7$ in the Na cell shows broad peaks at 2.6 V, 3.2 V, and 3.3 V. The initial peak at 2.6 V is very similar to the peak of $Na_2FeP_2O_7$ in the Na cell at 2.5 V. On comparing with the galvanostatic charge/discharge of behavior of $Na_{1.4}Li_{0.6}FeP_2O_7$, there appears a small plateau which is related to the small peak observed at 3.3 V. It can be further noticed that the CV analysis shows broad oxidation and reduction peaks, which are composed of different oxidation and reduction peaks similar to $Na_2FeP_2O_7$. The broad reduction peaks at around 2.75 V consist of three reduction peaks seen for $Na_2FeP_2O_7$. Lastly, Figure 8 (d) shows the CV for $Na_{1.4}Li_{0.6}FeP_2O_7$ in Li cell. The CV behavior is similar to that for $Na_2FeP_2O_7$ in Li cell except that the peaks are sharper and well defined. Two oxidation peaks are observed at around 3.1 V and 3.5 V, which relates to lithium extraction from different sites. During

reduction, again, two well-defined peaks are observed, which confirms the reversibility of the reaction and is consistent with charge/discharge behavior in Figure 4.

3. Conclusions

$Na_{2-x}Li_xFeP_2O_7$ (where x = 0, 0.6) was synthesized using a solid-state synthesis technique. The XRD spectra of $Na_{2-x}Li_xFeP_2O_7$ (where x = 0, 0.6) confirms the formation of phase pure materials, and the substitution of lithium does not alter the triclinic parent structure of $Na_2FeP_2O_7$. The TGA analysis shows that the substitution of lithium into $Na_2FeP_2O_7$ improves its thermal stability. It is noticed that $Na_{1.4}Li_{0.6}FeP_2O_7$ is electrochemically active and demonstrates decent cyclability in both the Li cell and Na cell. Although $Na_{1.4}Li_{0.6}FeP_2O_7$ currently suffers from low charge/discharge capacity and rate performance when compared to $Na_2FeP_2O_7$, its electrochemical performance can be improved with further investigations.

Supporting Information Summary

The supporting information contains the experimental section, detailing the synthesis procedure of $Na_{(2-x)}Li_xFeP_2O_7$ (x = 0, 0.6) Hybrid Cathodes. It also has structural, compositional, and thermal characterization technique parameters followed by a detailed electrode and cell fabrication procedure.

Acknowledgments

This publication was made possible by NPRP Grant#NPRP11S-1225-170128 from Qatar National Research Fund (a member of the Qatar Foundation). Statements made herein are solely the responsibility of the authors. Ramazan Kahraman and all the contributors would like to acknowledge the financial support of QU internal grant- QUCG-CENG-20/21-2. FE-SEM analysis was accomplished at the Central Laboratory Unit (CLU), Qatar University, Doha, Qatar.

Conflict of Interest

The authors declare no conflict of interest.

Keywords: Cyclic voltammetry · Charge and discharge capacity · Rate capability · Substitution · X-Ray Diffraction

[1] S. P. Guo, J. C. Li, Q. T. Xu, Z. Ma, H. G. Xue, *J. Power Sources.* **2017**, *361*, 285–299.
[2] M. D. Slater, D. Kim, E. Lee, C. S. Johnson, *Adv. Funct. Mater.* **2013**, *23*, 947–958.
[3] V. Etacheri, R. Marom, R. Elazari, G. Salitra, D. Aurbach, *Energy Environ. Sci.* **2011**, *4*, 3243–3262.
[4] D. Kim, S. H. Kang, M. Slater, S. Rood, J. T. Vaughey, N. Karan, M. Balasubramanian, C. S. Johnson, *Adv. Energy Mater.* **2011**, *1*, 333–336.
[5] U. Nisar, M. H. Gulied, R. A. Shakoor, R. Essehli, Z. Ahmad, A. Alashraf, R. Kahraman, S. Al-Qaradawi, A. Soliman, *RSC Adv.* **2018**, *8*, 32985–32991.
[6] P. R. Kumar, A. Kheireddine, U. Nisar, R. A. Shakoor, R. Essehli, R. Amin, I. Belharouak, *J. Power Sources.* **2019**, *429*, 149–155.
[7] U. Nisar, R. A. Shakoor, R. Essehli, R. Amin, B. Orayech, Z. Ahmad, P. R. Kumar, R. Kahraman, S. Al-Qaradawi, A. Soliman, *Electrochim. Acta.* **2018**, *292*, 98–106.
[8] J. Y. Hwang, S. T. Myung, Y. K. Sun, *Chem. Soc. Rev.* **2017**, *46*, 3529–3614.
[9] D. Saurel, B. Orayech, B. Xiao, D. Carriazo, X. Li, T. Rojo, *Adv. Energy Mater.* **2018**, *8*, 1703268.
[10] H. Kim, H. Kim, Z. Ding, M. H. Lee, K. Lim, G. Yoon, K. Kang, *Adv. Energy Mater.* **2016**, *6(19)*, 1600943.
[11] X. Lu, B. W. Kirby, W. Xu, G. Li, J. Y. Kim, J. P. Lemmon, V. L. Sprenkle, Z. Yang, *Energy Environ. Sci.* **2013**, *6*, 299–306.
[12] X. Lu, G. Xia, J. P. Lemmon, Z. Yang, *J. Power Sources.* **2010**, *195*, 2431–2442.
[13] B. L. Ellis, L. F. Nazar, *Curr. Opin. Solid State Mater. Sci.* **2012**, *16*, 168–177.
[14] B. Dunn, H. Kamath, J. M. Tarascon, *Science* **2011**, *334*, 928–935.
[15] P. Adelhelm, P. Hartmann, C. L. Bender, M. Busche, C. Eufinger, J. Janek, *Beilstein J. Nanotechnol.* **2015**, *6*, 1016–1055.
[16] U. Nisar, S. A. J. A. Al-Hail, R. K. Petla, R. A. Shakoor, R. Essehli, R. Kahraman, S. Y. AlQaradawi, D. K. Kim, I. Belharouak, M. R. Amin, *ACS Appl. Energy Mater.* **2019**, *2*, 7263–7271.
[17] S. M. Oh, S. T. Myung, J. Hassoun, B. Scrosati, Y. K. Sun, *Electrochem. Commun.* **2012**, *22*, 149–152.
[18] H. Kim, R. A. Shakoor, C. Park, S. Y. Lim, J. S. Kim, Y. N. Jo, W. Cho, K. Miyasaka, R. Kahraman, Y. Jung, J. W. Choi, *Adv. Funct. Mater.* **2013**, *23*, 1147–1155.
[19] Y. Kee, N. Dimov, A. Staikov, P. Barpanda, Y. C. Lu, K. Minami, S. Okada, *RSC Adv.* **2015**, *5*, 64991–64996.
[20] R. A. Shakoor, C. S. Park, A. A. Raja, J. Shin, R. Kahraman, *Phys. Chem. Chem. Phys.* **2016**, *18*, 3929–3935.
[21] H. Kim, I. Park, S. Lee, H. Kim, K. Y. Park, Y. U. Park, H. Kim, J. Kim, H. D. Lim, W. S. Yoon, K. Kang, *Chem. Mater.* **2013**, *25*, 3614–3622.
[22] S. Y. Lim, H. Kim, R. A. Shakoor, Y. Jung, J. W. Choi, *J. Electrochem. Soc.* **2012**, *159*, A1393.
[23] R. A. Shakoor, D. H. Seo, H. Kim, Y. U. Park, J. Kim, S. W. Kim, H. Gwon, S. Lee, K. Kang, *J. Mater. Chem.* **2012**, *22*, 20535–20541.
[24] P. R. Kumar, Y. H. Jung, S. A. Ahad, D. K. Kim, *RSC Adv.* **2017**, *7*, 21820–21826.
[25] R. Klee, P. Lavela, M. J. Aragón, R. Alcántara, J. L. Tirado, *J. Power Sources.* **2016**, *313*, 73–80.
[26] T. Jiang, G. Chen, A. Li, C. Wang, Y. Wei, *J. Alloys Compd.* **2009**, *478*, 604–607.
[27] P. Barpanda, G. Liu, M. Avdeev, A. Yamada, *ChemElectroChem.* **2014**, *1*, 1488–1491.
[28] C. A. J. Fisher, V. M. H. Prieto, M. S. Islam, *Chem. Mater.* **2008**, *20*, 5907–5915.
[29] Z. Chen, Y. Qin, K. Amine, Y. K. Sun, *J. Mater. Chem.* **2010**, *20*, 7606–7612.
[30] M. J. Aragón, B. León, T. Serrano, C. Pérez Vicente, J. L. Tirado, *J. Mater. Chem.* **2011**, *21*, 10102–10107.
[31] P.-F. Wang, Y. You, Y.-X. Yin, Y.-S. Wang, L.-J. Wan, L. Gu, Y.-G. Guo, *Angew. Chem.* **2016**, *128*, 7571–7575; *Angew. Chem. Int. Ed.* **2016**, *55*, 7445–7449.
[32] M. Gu, I. Belharouak, J. Zheng, H. Wu, J. Xiao, A. Genc, K. Amine, S. Thevuthasan, D. R. Baer, J. G. Zhang, N. D. Browning, J. Liu, C. Wang, *ACS Nano.* **2013**, *7(1)*, 760–767.
[33] W. R. Liu, Z. Z. Guo, W. S. Young, D. T. Shieh, H. C. Wu, M. H. Yang, N. L. Wu, *J. Power Sources.* **2005**, *140*, 139–144.
[34] J. Xu, H. Liu, Y. S. Meng, *Electrochem. Commun.* **2015**, *60*, 13–16.
[35] J. Xu, D. H. Lee, R. J. Clément, X. Yu, M. Leskes, A. J. Pell, G. Pintacuda, X.-Q. Yang, C. P. Grey, Y. S. Meng, *Chem. Mater.* **2014**, *26*, 1260–1269.
[36] N. Yabuuchi, R. Hara, M. Kajiyama, K. Kubota, T. Ishigaki, A. Hoshikawa, S. Komaba, *Adv. Energy Mater.* **2014**, *4(13)*, 1301453.
[37] B. Zhang, X. Ou, J. C. Zheng, C. Shen, L. Ming, Y. D. Han, J. L. Wang, S. E. Qin, *Electrochim. Acta.* **2014**, *133*, 1–7.
[38] J. Du, L. Jiao, Q. Wu, Y. Liu, Y. Zhao, L. Guo, Y. Wang, H. Yuan, *Electrochim. Acta.* **2013**, *103*, 219–225.
[39] H. Zhou, S. Upreti, N. A. Chernova, G. Hautier, G. Ceder, M. S. Whittingham, *Chem. Mater.* **2011**, *23*, 293–300.
[40] N. Furuta, S. I. Nishimura, P. Barpanda, A. Yamada, *Chem. Mater.* **2012**, *24*, 1055–1061.
[41] Y. H. Jung, C. H. Lim, J. H. Kim, D. K. Kim, *RSC Adv.* **2014**, *4*, 9799–9802.
[42] N. Ravet, M. Gauthier, K. Zaghib, J. B. Goodenough, A. Mauger, F. Gendron, C. M. Julien, *Chem. Mater.* **2007**, *19*, 2595–2602.

[43] A. Ait Salah, A. Mauger, K. Zaghib, J. B. Goodenough, N. Ravet, M. Gauthier, F. Gendron, C. M. Julien, *J. Electrochem. Soc.* **2006**, *153*, A1692.
[44] H. Kim, S. Lee, Y. U. Park, H. Kim, J. Kim, S. Jeon, K. Kang, *Chem. Mater.* **2011**, *23*, 3930–3937.
[45] L. G. Chagas, D. Buchholz, L. Wu, B. Vortmann, S. Passerini, *J. Power Sources.* **2014**, *247*, 377–383.
[46] N. V. Kosova, A. A. Shindrov, **2019**, 5829–5838.
[47] E. De La Llave, E. Talaie, E. Levi, P. K. Nayak, M. Dixit, P. T. Rao, P. Hartmann, F. Chesneau, D. T. Major, M. Greenstein, D. Aurbach, L. F. Nazar, *Chem. Mater.* **2016**, *28*, 9064–9076.
[48] Y. Zhao, K. R. Adair, X. Sun, *Energy Environ. Sci.* **2018**, *11*, 2673–2695.
[49] P. Barpanda, T. Ye, S. I. Nishimura, S. C. Chung, Y. Yamada, M. Okubo, H. Zhou, A. Yamada, *Electrochem. Commun.* **2012**, *24*, 116–119.
[50] J. M. Clark, P. Barpanda, A. Yamada, M. S. Islam, *J. Mater. Chem. A.* **2014**, *2*, 11807–11812.
[51] G. Longoni, J. E. Wang, Y. H. Jung, D. K. Kim, C. M. Mari, R. Ruffo, *J. Power Sources.* **2016**, *302*, 61–69.

Submitted: September 17, 2020
Accepted: October 5, 2020